

Laser line-shape effects in resonance fluorescence

A. T. Georges*

Department of Physics, University of Toronto, Toronto, Ontario, Canada M5S 1A7

S. N. Dixit

Department of Physics, University of Southern California, Los Angeles, California 90007

(Received 27 August 1980)

The effects of different laser line shapes on the intensity and spectrum of resonance fluorescence from a two-level atom are investigated. The laser model considered is that of an ideal single-mode laser operating high above threshold, with constant amplitude and undergoing phase-frequency fluctuations analogous to Brownian motion. As the correlation time of the frequency fluctuations increases from zero to infinity, the laser line shape changes from Lorentzian to Gaussian in a continuous way. It is shown that for intermediate and strong fields, the average intensity of fluorescence in the case of a resonant broadband Lorentzian line shape is higher than that in the case of a Gaussian line shape with the same bandwidth and total power. This is in contrast to the weak-field case where the higher peak power of the Gaussian line shape makes it more effective than the Lorentzian line shape. It is also shown that in the case of a nonzero frequency correlation time (non-Lorentzian line shape) the intensity of fluorescence undergoes non-Markovian fluctuations. In relation to the spectrum of resonance fluorescence, it is shown that as the line shape is varied from Lorentzian to Gaussian the following changes take place: In the case of off-resonance excitation, the asymmetry of the spectrum decreases. In the case of resonant excitation, the center-peak to side-peak height ratio for the triplet structure increases. Moreover, the recently predicted center-line dip, which develops in the spectrum in the case of broadband excitation when the Rabi frequency and the bandwidth are nearly equal, becomes increasingly deeper.

I. INTRODUCTION

During the last four years, a large number of papers have been written dealing with the effects of laser-field fluctuations on the resonance fluorescence from a two-level atom.¹⁻¹⁰ The earlier of these papers dealt only with phase fluctuations,¹⁻⁶ while the later ones treated amplitude fluctuations as well.⁷⁻¹⁰ Three different Markovian models have been used for the field: (i) a phase-diffusion field,¹⁻⁶ (ii) a chaotic field,⁷⁻¹⁰ and (iii) a Gaussian-amplitude field.^{9,10} Many interesting new results have come out of these investigations. It has been shown, for example, that the intensity of resonance fluorescence in the presence of a field with amplitude fluctuations is less than that in the presence of a field with only phase fluctuations, having the same average power and bandwidth. It has also been shown that field fluctuations have a strong influence on the spectrum of resonance fluorescence. In the case of a phase-diffusion field, the finite bandwidth broadens the three-peak strong-field spectrum, and when the bandwidth is nearly equal to the Rabi frequency the spectrum exhibits a symmetric doublet structure.⁹ In the case of amplitude fluctuations, on the other hand, the side bands of the strong-field spectrum are suppressed and tend to reproduce the probability distribution for the amplitude of the field.⁷⁻⁹

The three model fields mentioned above all have Lorentzian line shapes, owing to the Markovian

character of their phase and amplitude fluctuations. Realistic laser line shapes, however, fall off much faster than Lorentzian line shapes. Although the effects found in the case of fluctuating fields with Lorentzian line shapes¹⁻¹⁰ should occur also in the case of fields with non-Lorentzian line shapes, one would expect some quantitative differences. For example, in the case of off-resonance excitation a Gaussian line shape, which falls off much faster than a Lorentzian, would excite fewer atoms than a Lorentzian line shape with the same total power and bandwidth. In this paper, we present for the first time a rigorous treatment of resonance fluorescence in the presence of a fluctuating laser field with a non-Lorentzian line shape. The laser model considered here was employed recently in the investigation of laser line-shape effects in optical double resonance.^{11,12} It corresponds to an ideal single-mode laser operating high above threshold, having a constant amplitude and undergoing phase-frequency fluctuations analogous to Brownian motion.^{13,14} As the correlation time of the Gaussian-Markovian frequency fluctuations increases from zero to infinity, the laser line shape changes from Lorentzian to Gaussian in a continuous way. We should point out that the special case of zero correlation time for the frequency fluctuations corresponds to the phase-diffusion model mentioned above. The non-Lorentzian laser line shape, in the general case of a non-zero-frequency correlation time is associated with the non-Markovian

character of the phase fluctuations.

The interaction of a two-level atom with this stochastic laser field is described in the context of the density-matrix formalism. To solve the stochastic equations of motion for the atomic density-matrix operator and its quantum correlation functions, we use a recently developed method for treating Markovian-field fluctuations.^{7-9,12} In this method, the Markovian-frequency fluctuations are described statistically in terms of the marginal and conditional probability densities. The stochastic density-matrix operator and its correlation functions are then expanded in terms of the eigenfunctions of the conditional averaging integral. This series expansion in terms of stochastic eigenfunctions reduces the stochastic equations of motion into a set of deterministic equations for the expansion coefficients. The interesting point about this method, which takes into account the statistics of the field to all orders, is that it gives not only the average solution but the complete stochastic solution as well. In Sec. II we describe the statistics of the laser field, and in Secs. III and IV we investigate their effects on the intensity and the spectrum of resonance fluorescence.

II. STATISTICS OF THE LASER FIELD

The laser field considered in this paper is that of an ideal single-mode laser operating high above threshold.¹³ Neglecting very small amplitude fluctuations, the electric field can be written as

$$E(t) = \mathcal{E}_0 e^{-i[\omega_0 t + \phi(t)]} + c.c., \quad (1)$$

where \mathcal{E}_0 is a constant amplitude, ω_0 the center frequency of the spectrum, and $\phi(t)$ the phase which undergoes Brownian-motion-type fluctua-

$$\langle\langle \phi(t_1)\phi(t_2) \rangle\rangle = (\gamma_D/2\beta)(2\beta t_2 - 1 + e^{-\beta t_1} + e^{-\beta t_2} - e^{-\beta(t_1+t_2)}), \quad (5)$$

where $t_1 > t_2$ and the double angular brackets denote stochastic average over both ϕ and ν . Using the equation above we can show that

$$\langle\langle [\phi(t_1) - \phi(t_2)][\phi(t_2) - \phi(t_3)] \rangle\rangle = (\gamma_D/2\beta)(1 - e^{-\beta(t_1-t_2)} + e^{-\beta(t_1-t_3)} - e^{-\beta(t_2-t_3)}), \quad (6)$$

where $t_1 > t_2 > t_3$. Therefore, the phase increments $\phi(t_1) - \phi(t_2)$ and $\phi(t_2) - \phi(t_3)$ are correlated and it is only in the limit $\beta \rightarrow \infty$ that they become statistically uncorrelated and independent. In this limit Brownian motion reduces to a Wiener-Levy process and the phase $\phi(t)$ becomes a Markovian process, with the conditional probability density $f(\phi_1, t_1 | \phi_2, t_2)$ satisfying the diffusion equation $\partial f / \partial t_1 = (\gamma_D/2) \partial^2 f / \partial \phi_1^2$. This special case is known as the phase-diffusion model (PDM).¹³ The normalized laser spectrum is the Fourier transform of the field correlation function

The frequency fluctuations $\nu(t) = d\phi(t)/dt$ are analogous to the fluctuations in the velocity of a free particle in Brownian motion and obey Gaussian-Markovian statistics.^{14,15} The mean value of $\nu(t)$ is zero and its autocorrelation is given by

$$\langle \nu(t_1)\nu(t_2) \rangle = \frac{1}{2}\beta\gamma_D e^{-\beta|t_1-t_2|}, \quad (2)$$

where $1/\beta$ is the correlation time and $(\beta\gamma_D/2)^{1/2}$ the standard deviation of the frequency fluctuations. In terms of basic laser parameters, 2β is equal to the sum of the decay rates of the cavity and the lasing transition, while γ_D depends on the laser medium and is inversely proportional to the output power of the laser.¹³ The marginal probability density for $\nu(t)$ is given by^{14,15}

$$f(\nu) = \frac{e^{-\nu^2/(2\beta\gamma_D)}}{(\pi\beta\gamma_D)^{1/2}}, \quad (3)$$

and the conditional probability density by

$$f(\nu_1, t_1 | \nu_2, t_2) = \frac{\exp\left(\frac{(\nu_1 - r\nu_2)^2}{\beta\gamma_D(1-r^2)}\right)}{[\pi\beta\gamma_D(1-r^2)]^{1/2}}, \quad t_1 > t_2 \quad (4)$$

where $r = \langle \nu(t_1)\nu(t_2) \rangle / \langle \nu^2(t) \rangle = e^{-\beta(t_1-t_2)}$ is the correlation coefficient for the frequency fluctuations. Since $\nu(t)$ is a Markovian process, Eqs. (2)-(4) completely determine its statistics.

The phase $\phi(t)$, being the integral of a Gaussian-Markovian process, is also a Gaussian process whose future is independent of the past and depends only on the present values of $\nu(t)$ and itself. We should point out that $\phi(t)$ alone is not a Markovian process, but together with $\nu(t)$ they form a two-dimensional Gaussian-Markovian process.¹⁴ The autocorrelation of $\phi(t)$ is given by

$$\begin{aligned} R(\tau) &= \langle\langle \exp[i\phi(t+\tau) - i\phi(t)] \rangle\rangle \\ &= \left\langle \exp\left(\int_0^\tau \nu(t') dt'\right) \right\rangle \\ &= \exp\left[-\frac{\gamma_D}{2}\left(|\tau| + \frac{e^{-\beta|\tau|} - 1}{\beta}\right)\right], \end{aligned} \quad (7)$$

and is given by

$$L(\omega - \omega_0) = \frac{e^x}{\pi\beta} \operatorname{Re} \left[x^{-x+i(\omega-\omega_0)/\beta} \gamma \left(x - i \frac{\omega - \omega_0}{\beta}, x \right) \right], \quad (8)$$

where $x = \gamma_D/(2\beta)$ and $\gamma(a, x)$ is the incomplete

gamma function.¹⁶ The expression for the spectrum $L(\omega - \omega_0)$ is a complicated function of β , γ_D , and ω . A qualitative picture of the spectrum can, however, be obtained from the time dependence of the correlation $R(\tau)$, which has a simpler form. Since for very short times ($\tau \ll 1/\beta$; γ_D arbitrary) $R(\tau) \approx e^{-\beta\gamma_D\tau^2/4}$, for frequencies $|\omega - \omega_0| \gg \beta$ the spectrum is given by $L(\omega - \omega_0) \approx f(\omega - \omega_0)$; that is, for those frequencies in the Gaussian distribution [Eq. (3)] for which one observes many cycles over a frequency correlation time ($|\omega - \omega_0|/\beta \gg 1$), the spectral weight is the same as the statistical weight. For all the other frequencies, which are not resolved within a correlation time, the spectral weight is determined by the overall phase drift which they produce. In the case of $\beta \gg \gamma_D$, the central part of the spectrum for $|\omega - \omega_0| \ll \beta$ is given by the Fourier transform of $R(\tau) \approx \exp[\gamma_D/(2\beta)] \exp(-\gamma_D|\tau|/2)$, which is Lorentzian with full width at half-maximum (FWHM) $\gamma = \gamma_D$.

Therefore, for $\beta \gg \gamma_D$ the spectrum $L(\omega - \omega_0)$ consists of a Lorentzian peak with Gaussian wings for $|\omega - \omega_0| \gg \beta$. As β decreases (γ_D assumed fixed) the Gaussian portion of the spectrum increases and for $\beta \ll \gamma_D$ the entire spectrum essentially becomes Gaussian with FWHM $\gamma = 2(\ln 2\beta\gamma_D)^{1/2}$. Note that although according to ideal laser theory $\beta > \gamma_D$, in this paper we will also consider the case of $\beta < \gamma_D$ as a mathematical model for Gaussian line shapes.

The N th-order field correlation function is given by¹⁵

$$\begin{aligned} & \langle\langle e^{i\phi(t_1)} e^{-i\phi(t_2)} \dots e^{i\phi(t_{2N-1})} e^{-i\phi(t_{2N})} \rangle\rangle \\ & = \exp\left(-\frac{1}{2} \sum_{n=1}^{2N} \sum_{m=1}^{2N} (-1)^{n+m} \langle\langle \phi(t_n) \phi(t_m) \rangle\rangle\right). \end{aligned} \quad (9)$$

Evaluating the equation above in the case of $N=2$ we obtain

$$\begin{aligned} & \langle\langle e^{i\phi(t_1)} e^{-i\phi(t_2)} e^{i\phi(t_3)} e^{-i\phi(t_4)} \rangle\rangle = \langle\langle e^{i\phi(t_1)} e^{-i\phi(t_2)} \rangle\rangle \langle\langle e^{i\phi(t_3)} e^{-i\phi(t_4)} \rangle\rangle \\ & \quad \times \exp\left(-\frac{\gamma_D}{2\beta} (e^{-\beta(t_1-t_4)} - e^{-\beta(t_1-t_3)} - e^{-\beta(t_2-t_4)} + e^{-\beta(t_2-t_3)})\right), \end{aligned} \quad (10)$$

where $t_1 > t_2 > t_3 > t_4$. As we can see, the second-order field correlation does not factorize exactly into time-ordered first-order field correlations. This is true for all higher-order correlations and is connected to the fact that the phase increments are not statistically independent. It is only in the limit of $\beta \rightarrow \infty$ (PDM) that the factorization into first-order correlations becomes exact. As shown in Ref. 17, because of this nonfactorization, the decorrelation of atomic and field variables in an atom-field interaction is not valid for the laser field considered here, except in the case of $\beta \rightarrow \infty$.

Having described the statistical and spectral properties of the laser field, we now outline the method used in averaging the equations of motion for the density-matrix operator and its quantum correlation functions. The equations are written in terms of the instantaneous frequency of the field $\omega_0 + \nu(t)$, and averaged over $\nu(t)$ using the method developed in Ref. 9 for fields with Markovian variables (amplitude, phase, and frequency). The average is carried out by expanding the atomic variables in terms of the orthonormal eigenfunctions of the conditional averaging integral. The conditional probability density $f(\nu_1, t_1 | \nu_2, t_2)$ is a generating function for Hermite polynomials and it can be shown that

$$\langle H_N(\nu_1/(\beta\gamma_D)^{1/2}) | \nu_2, t_2 \rangle \equiv \int_{-\infty}^{\infty} H_N(\nu_1/(\beta\gamma_D)^{1/2}) f(\nu_1, t_1 | \nu_2, t_2) d\nu_1 = e^{-N\beta(t_1-t_2)} H_N(\nu_2/(\beta\gamma_D)^{1/2}), \quad (11)$$

where $H_N(x)$ is a Hermite polynomial.¹⁶ Therefore, $H_N(\nu_1/(\beta\gamma_D)^{1/2})$ is an eigenfunction of the conditional averaging integral with eigenvalue $e^{-N\beta(t_1-t_2)}$. The marginal average of the eigenfunctions is $\langle H_N(\nu/(\beta\gamma_D)^{1/2}) \rangle = \delta_{N0}$ and their correlation function, $\langle H_N(\nu(t_1)/(\beta\gamma_D)^{1/2}) H_M(\nu(t_2)/(\beta\gamma_D)^{1/2}) \rangle = e^{-N\beta|t_1-t_2|} \delta_{MN}$, is the same as their eigenvalue.¹⁸ Note that the correlation time $(1/N\beta)$ of the stochastic eigenfunctions decreases with increasing N , indicating more rapid fluctuations. This is expected since the higher-order polynomials involve higher powers of $\nu(t)$. In a series expansion of a stochas-

tic function of $\nu(t)$ in terms of $H_N(\nu(t)/(\beta\gamma_D)^{1/2})$, the stochastic Hermite polynomials play the same role as the sinusoids in a Fourier-series expansion, with the correlation time $(1/N\beta)$ being analogous to the period of the N th harmonic. By expanding the density-matrix operator and its quantum correlation functions in terms of the eigenfunctions of the conditional averaging integral, the problem of finding the solution of their stochastic equations of motion reduces to the simpler problem of finding the solution of the deterministic system of equations for the expansion coefficients.

III. INTENSITY OF RESONANCE FLUORESCENCE

In this section we calculate the average intensity of the fluorescent light emitted from a two-level atom interacting with the stochastic laser field described in Sec. II. The two-level atom is characterized by the transition frequency ω_{21} , the electric-dipole moment μ_{12} , and the spontaneous decay rate Γ from the excited level ($|2\rangle$) to the ground level ($|1\rangle$). The interaction is described in terms of the atomic density matrix $\rho(t)$ in the rotating-wave approximation. Introducing the slowly varying amplitudes $\sigma'_{ij}(t)$, defined by

$$\rho_{12}(t) = \sigma'_{12}(t)e^{-i[\omega_0 t + \phi(t)]}, \quad \rho_{21}(t) = \sigma'_{21}(t)e^{i[\omega_0 t + \phi(t)]}, \quad \rho_{ii}(t) = \sigma'_{ii}(t),$$

the equations of motion for the density-matrix elements take the form

$$\frac{d}{dt} \begin{pmatrix} \sigma'_{22}(t) \\ \sigma'_{11}(t) \\ \sigma'_{12}(t) \\ \sigma'_{21}(t) \end{pmatrix} = \begin{pmatrix} -\Gamma & 0 & -i\frac{1}{2}\omega_R & i\frac{1}{2}\omega_R \\ \Gamma & 0 & i\frac{1}{2}\omega_R & -i\frac{1}{2}\omega_R \\ -i\frac{1}{2}\omega_R & i\frac{1}{2}\omega_R & i[\Delta + \nu(t)] - \Gamma/2 & 0 \\ i\frac{1}{2}\omega_R & -i\frac{1}{2}\omega_R & 0 & -i[\Delta + \nu(t)] - \Gamma/2 \end{pmatrix} \begin{pmatrix} \sigma'_{22}(t) \\ \sigma'_{11}(t) \\ \sigma'_{12}(t) \\ \sigma'_{21}(t) \end{pmatrix}, \quad (12)$$

where $\Delta = \omega_0 - \omega_{21}$ is the detuning from resonance and $\omega_R = 2\hbar^{-1}\mu_{12}\mathcal{E}_0$ the Rabi frequency. If we now integrate these equations with initial conditions $\sigma'_{11}(0) = 1$, $\sigma'_{22}(0) = \sigma'_{12}(0) = \sigma'_{21}(0) = 0$, we obtain the integral equations

$$n(t) = -1 - i\omega_R \int_0^t e^{\Gamma(t_1-t)} [\sigma'_{12}(t_1) - \sigma'_{12}^*(t_1)] dt_1, \quad (13)$$

$$\sigma'_{12}(t) = i \int_0^t e^{(-i\Delta + \Gamma/2)(t_1-t)} [\nu(t_1)\sigma'_{12}(t_1) - \frac{1}{2}\omega_R n(t_1)] dt_1, \quad (14)$$

where $n(t) = \sigma'_{22}(t) - \sigma'_{11}(t)$ is the population inversion and we use the normalization $\sigma'_{11}(t) + \sigma'_{22}(t) = 1$. To average these stochastic integral equations over the frequency fluctuations first we expand $n(t)$ and

$\sigma'_{12}(t)$ in terms of the eigenfunctions of the conditional averaging integral; for example,

$$n(t) = \sum_{N=0}^{\infty} \langle n(t) \rangle_N H_N \left(\frac{\nu(t)}{(\beta\gamma_D)^{1/2}} \right), \quad (15)$$

where the averages $\langle n(t) \rangle_N \equiv \langle H_N(\nu(t))/(\beta\gamma_D)^{1/2} n(t) \rangle$ are expansion coefficients. Note that since $H_0(x) = 1$, the zeroth-order coefficient in such an expansion is the average value of the expanded stochastic function. Next, multiplying Eqs. (13) and (14) by $H_N(\nu(t))/(\beta\gamma_D)^{1/2}$ and the joint probability density $f(\nu, \nu_1; t, t_1) = f(\nu, t | \nu_1, t_1)f(\nu_1)$, and then integrating over the random variables ν and ν_1 , we obtain the following equations for the deterministic expansion coefficients:

$$\langle n(t) \rangle_N = -\delta_{N0} - i\omega_R \int_0^t e^{(\Gamma + N\beta)(t_1-t)} [\langle \sigma'_{12}(t_1) \rangle_N - \langle \sigma'_{12}^*(t_1) \rangle_N] dt_1, \quad (16)$$

$$\langle \sigma'_{12}(t) \rangle_N = i \int_0^t e^{(-i\Delta + \Gamma/2 + N\beta)(t_1-t)} \left\{ (\beta\gamma_D)^{1/2} \left[\left(\frac{N+1}{2} \right)^{1/2} \langle \sigma'_{12}(t_1) \rangle_{N+1} + \left(\frac{N}{2} \right)^{1/2} \langle \sigma'_{12}(t_1) \rangle_{N-1} \right] - \frac{1}{2}\omega_R \langle n(t_1) \rangle_N \right\} dt_1, \quad (17)$$

where $\langle \sigma'_{12}(t) \rangle_N \equiv \langle H_N(\nu(t))/(\beta\gamma_D)^{1/2} \sigma'_{12}(t) \rangle$. In deriving these two equations we have used Eq. (11), the orthogonality relation for the Hermite polynomials and the recursion relation^{16,18}

$$xH_N(x) = \left[\frac{1}{2}(N+1) \right]^{1/2} H_{N+1}(x) + \left(\frac{1}{2}N \right)^{1/2} H_{N-1}(x). \quad (18)$$

The integral Eqs. (16) and (17) can be solved by Laplace transform. The Laplace transforms of the expansion coefficients satisfy the infinite algebraic system of equations

$$(s + \Gamma + N\beta)L\langle n(t) \rangle_N = -\frac{(s + \Gamma)}{s} \delta_{N0} - i\omega_R [L\langle \sigma'_{12}(t) \rangle_N - L\langle \sigma'_{12}^*(t) \rangle_N], \quad (19)$$

$$(s - i\Delta + \Gamma/2 + N\beta)L\langle \sigma'_{12}(t) \rangle_N = i \left[\frac{1}{2}\beta\gamma_D(N+1) \right]^{1/2} L\langle \sigma'_{12}(t) \rangle_{N+1} + i \left[\frac{1}{2}\beta\gamma_D N \right]^{1/2} L\langle \sigma'_{12}(t) \rangle_{N-1} - \frac{1}{2}\omega_R L\langle n(t) \rangle_N, \quad (20)$$

where L and s denote the Laplace transform operator and its argument, respectively. Eliminating $L\langle n(t) \rangle_N$ from the equations above and defining the column vectors $X_N(s) \equiv [L\langle \sigma'_{12}(t) \rangle_N, L\langle \sigma'_{12}^*(t) \rangle_N]$ and $Y \equiv (i\frac{1}{2}\omega_R, i\frac{1}{2}\omega_R)$ we obtain the matrix recursion relation

$$-i\sqrt{a}NX_{N-1}(s) + b_N X_N(s) - i[a(N+1)]^{1/2}X_{N+1}(s) = Y \delta_{N0}, \quad N=0, 1, \dots, \quad (21)$$

where $a = \beta\gamma_D/2$ and b_N is a 2×2 complex matrix with elements

$$\begin{aligned} b_N |_{11} &= s - i\Delta + \Gamma/2 + N\beta + \frac{1}{2}\omega_R^2/(\Gamma + N\beta), \\ b_N |_{22} &= s + i\Delta + \Gamma/2 + N\beta + \frac{1}{2}\omega_R^2/(\Gamma + N\beta), \\ b_N |_{12} &= -b_N |_{21} = -\frac{1}{2}\omega_R^2/(\Gamma + N\beta). \end{aligned}$$

The solution for the column vector $X_0(s) = (L\langle \sigma'_{12}(t) \rangle, L\langle \sigma'_{12}^*(t) \rangle)$ can be written in terms of a matrix continued fraction

$$X_0(s) = \frac{1}{b_0 + \frac{a}{b_1 + \frac{2a}{b_2 + \frac{3a}{b_3 + \dots}}}} Y \quad (22)$$

This expression can be evaluated numerically using the iteration method for evaluating continued fractions.^{12,16} The time-dependent averages $\langle \sigma'_{12}(t) \rangle$ and $\langle \sigma'_{12}^*(t) \rangle$ can then be evaluated by taking the inverse Laplace transform of Eq. (22), numerically. In this paper, however, we consider only the steady-state solution which can be obtained from the relation

$$\lim_{s \rightarrow 0} sX_0(s) = (\langle \sigma'_{12}(t = \infty) \rangle, \langle \sigma'_{12}^*(t = \infty) \rangle).$$

The steady-state value of the average population of the excited state is obtained from the relation

$$\langle \sigma'_{22} \rangle = -i \frac{\omega_R}{\Gamma} (\langle \sigma'_{12} \rangle - \langle \sigma'_{12}^* \rangle). \quad (23)$$

The average intensity of the fluorescent light is proportional to $\langle \sigma'_{22} \rangle$. If the continued fraction in Eq. (22) is truncated after b_1 , Eq. (23) reduces to

$$\langle \sigma'_{22} \rangle \approx \frac{S/2}{1+S}, \quad (24)$$

where the saturation parameter S is given by

$$S = \frac{\omega_R^2}{\Gamma} \frac{\frac{1}{2}(\Gamma + W)}{\Delta^2 \left(1 - \frac{W}{\Gamma + 2\beta}\right)^2 + \frac{1}{4}(\Gamma + W)^2} \quad (25)$$

with

$$W = \gamma_D \frac{\beta(\Gamma/2 + \beta)}{\Delta^2 + (\Gamma/2 + \beta)^2}. \quad (26)$$

In the limit of $\beta \rightarrow \infty$ (PDM), Eq. (24) is exact. For realistic finite values of β , however, Eq. (24) is a good approximation only if $\frac{1}{2}\beta\gamma_D \ll \Delta^2 + (\Gamma/2 + \beta)^2$ and $\omega_R \ll (\Gamma + \beta)$. These conditions insure that the fluctuations in σ'_{22} are negligible compared to the average value. From the first condition above we can see that if $\beta \gg \gamma_D$, in which case the spectrum is Lorentzian with Gaussian wings, Eq. (24) is a good approximation for arbitrary detunings. This is also true for $\frac{1}{2}\beta\gamma_D \ll (\Gamma/2)^2$, that is when the standard deviation of the frequency fluctuations is much smaller than the atomic linewidth (quasi-monochromatic field). If, however, $\frac{1}{2}\beta\gamma_D \gg (\Gamma/2 + \beta)^2$, in which case $\beta \ll \gamma_D$ and therefore the whole spectrum is essentially Gaussian, then Eq. (24) is a good approximation only for detunings much larger than the width of the spectrum ($\Delta^2 \gg \frac{1}{2}\beta\gamma_D$). For excitation far off resonance [$\Delta \gg \Gamma/2 + \beta, (\frac{1}{2}\beta\gamma_D)^{1/2}$], Eqs. (24)–(26) show that as the detuning is increased the incoherent part of the excitation decreases much faster than the coherent part. Note that the coherent part of the excitation is the part which depends only on the total intensity of the field, while the incoherent part depends on the bandwidth of field as well and vanishes in the case of monochromatic fields. In the approximation of Eq. (24), the incoherent part decreases as Δ^{-4} , while the coherent part as expected, decreases as Δ^{-2} . Note that for an ideal Lorentzian line shape ($\beta \rightarrow \infty$) the incoherent part decreases as Δ^{-2} , and for $\gamma_D > \Gamma$ it is larger than the coherent part. An ideal Lorentzian laser line shape is, however, unrealistic in the case of far-off-resonance excitation. Exactly on resonance, the averages $\langle \sigma'_{12} \rangle_N - \langle \sigma'_{12}^* \rangle_N$, $N=0, 2, 4, \dots$, satisfy a three-term recursion relation and the steady-state value of the average $\langle \sigma'_{22} \rangle$ can be expressed in terms of a continued fraction

$$\langle \sigma'_{22} \rangle = \frac{S/2}{1+S} \frac{1}{1 - \frac{C_0}{1 - \frac{C_2}{1 - \dots}}}, \quad (27)$$

where S is the saturation parameter given in Eq. (25) with $\Delta=0$ and

$$C_N = \frac{(\frac{1}{2}\beta\gamma_D)^2(N+1)(N+2)}{[\Gamma/2 + (N+1)\beta]^2 d_N d_{N+2}}, \quad (28)$$

with

$$\begin{aligned} d_N &= \frac{\Gamma}{2} + N\beta + \frac{\omega_R^2}{\Gamma + N\beta} + \frac{\frac{1}{2}\beta\gamma_D N}{\Gamma/2 + (N-1)\beta} \\ &\quad + \frac{\frac{1}{2}\beta\gamma_D(N+1)}{\Gamma/2 + (N+1)\beta}. \end{aligned} \quad (29)$$

The continued fraction in Eq. (27) is more simple to evaluate than the matrix continued fraction in Eq. (22).

Intensity correlation

The expansion of the stochastic density-matrix elements in terms of Hermite polynomials [see Eq. (15)] allow us also to evaluate multitime correlation functions. As an example we evaluate the two-time intensity correlation³ $\langle\langle \hat{\sigma}_{21}(t) \hat{\sigma}_{21}(t+\tau) \rangle\rangle$, where the inner and outer brackets denote quantum and field average, respectively. As has been shown in Ref. 10, this correlation reduces to $\langle\langle \hat{\sigma}_{22}(t) \hat{\sigma}_{22}(t+\tau | t, |1\rangle) \rangle\rangle = \langle\sigma_{22}(t) \sigma_{22}(t+\tau | t, |1\rangle)\rangle$, where $\sigma_{22}(t+\tau | t, |1\rangle)$ is the population of state $|2\rangle$ at time $t+\tau$, given that the atom is in state $|1\rangle$ at time t . Using Eq. (11) and the orthogonality relation for Hermite polynomials we can show that

$$\langle\sigma_{22}(t) \sigma_{22}(t+\tau | t, |1\rangle)\rangle = \sum_{N=0}^{\infty} \langle\sigma_{22}(t)\rangle_N \langle\sigma_{22}(t+\tau | t, |1\rangle)\rangle_N e^{-N\beta\tau}, \quad (30)$$

where the averages $\langle\sigma_{22}(t)\rangle_N = \frac{1}{2}(\hat{\sigma}_{N0} + \langle n(t)\rangle_N)$ can be evaluated from Eqs. (19) and (22). Note that for $\tau=0$, $\langle\sigma_{22}(t+\tau | t, |1\rangle)\rangle_N = 0$ and the intensity correlation vanishes, thus exhibiting antibunching.^{3,10} In the phase-diffusion limit ($\beta \rightarrow \infty$) the averages $\langle\sigma_{22}(t)\rangle_N$, $\langle\sigma_{22}(t+\tau | t, |1\rangle)\rangle_N$, $N > 0$, are zero and therefore $\langle\sigma_{22}(t) \sigma_{22}(t+\tau | t, |1\rangle)\rangle = \langle\sigma_{22}(t)\rangle \langle\sigma_{22}(t+\tau | t, |1\rangle)\rangle$. Thus, the two-time intensity correlation factorizes into a product of average intensities, in agreement with previous work.³ In the general case ($\beta \neq \infty$), however, this factorization is not valid as can be seen from Eq. (30). The physical interpretation for this difference is the following. Pure phase fluctuations ($\beta \rightarrow \infty$) do not produce any fluctuations in the intensity of fluorescence. This is because for $\beta \rightarrow \infty$ all the frequencies in the exciting spectrum act on the atom simultaneously. For finite values of β , however, the different frequencies act on the atom randomly and, therefore, produce fluctuations in the intensity of fluorescence. Since the intensity correlation [Eq. (30)] is a sum of exponentials with different decay rates and amplitudes, the intensity fluctuations are non-Markovian. The effect of the frequency fluctuations in the laser field is also exhibited in the quantum averaged population of state $|2\rangle$. The standard deviation of $\sigma_{22}(t)$ is given by

$$[\langle\sigma_{22}^2(t)\rangle - \langle\sigma_{22}(t)\rangle^2]^{1/2} = \left(\sum_{N=1}^{\infty} \langle\sigma_{22}(t)\rangle_N^2 \right)^{1/2}. \quad (31)$$

Note that for $\beta \rightarrow \infty$, the averages $\langle\sigma_{22}(t)\rangle_N$, $N > 0$ vanish and, therefore, the standard deviation of $\sigma_{22}(t)$ is zero. This shows that pure phase fluctuations do not produce fluctuations in the quantum-averaged populations.

Numerical calculations and discussion

To illustrate the influence of the laser line shape on the average intensity of resonance fluorescence, we have performed numerical calculations for three different values of the line-shape parameter β , $\beta = \infty$, $\beta = \Gamma$, and $\beta = 0.1\Gamma$. The value of the diffusion constant γ_D has been chosen so that for each value of β the FWHM of the spectrum takes three characteristic values, $\gamma = 0.1\Gamma$ (narrowband), $\gamma = \Gamma$, and $\gamma = 10\Gamma$ (broadband). In the actual calculations, the atomic linewidth Γ is set equal to unity. For $\beta = \infty$ the line shape is ideal Lorentzian, while for $\beta = 0.1\Gamma$ the lineshape is essentially Gaussian. In the case of $\beta = \Gamma$, the line shape consists of a Lorentzian peak with Gaussian wings. Figure 1 shows the ratio of the stationary average population $\langle\sigma'_{22}\rangle$ for $\beta = 0.1\Gamma$ (solid line) and $\beta = \Gamma$ (dashed line) to the average population $\langle\sigma'_{22}\rangle^L$ for a Lorentzian line shape ($\beta = \infty$) as a function of the Rabi frequency under exact resonance. As can be seen, for very weak fields a line shape which falls off faster than a Lorentzian produces a larger excitation than a Lorentzian line shape with the same FWHM and total power. Even in the narrowband case ($\gamma = 0.1\Gamma$), a Gaussian spectrum excites ~8% more atoms than a Lorentzian spectrum ($\omega_R \ll \Gamma$), while for $\gamma = \Gamma$ this difference becomes 38%. For broadband excitation ($\gamma \gg \Gamma$) in the weak-field limit, the ratio of the populations excited by a Gaussian and a Lorentzian spectrum goes to the limit $(\pi \ln 2)^{1/2} \approx 1.48$, which corresponds to the ratio of the peak of a Gaussian spectrum to that of a Lorentzian spectrum with the same FWHM and power. If $\gamma \leq \Gamma$, as the intensity of the field increases, the ratio $\langle\sigma'_{22}\rangle / \langle\sigma'_{22}\rangle^L$ decreases monotonically to unity because of saturation. If, however, $\gamma > \Gamma$ the ratio decreases to a minimum val-

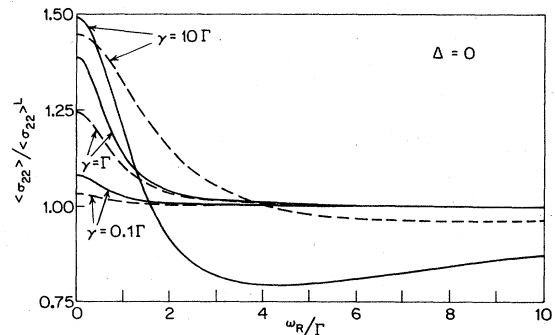


FIG. 1. Plot of the stationary excited-state population $\langle\sigma'_{22}\rangle$ for $\beta = \Gamma$ (dashed line) and $\beta = 0.1\Gamma$ (solid line), normalized to the population $\langle\sigma'_{22}\rangle^L$ for $\beta = \infty$, as a function of the ratio ω_R/Γ of the Rabi frequency to the spontaneous decay rate. The detuning of the fields from resonance is zero and the laser bandwidth (γ) takes three different values.

ue below unity and then goes to unity in the limit of $\omega_R/\Gamma \rightarrow \infty$. Therefore, a strong broadband Lorentzian spectrum excites more atoms than a Gaussian spectrum. The reason for the broadband Gaussian spectrum becoming less effective than the Lorentzian spectrum at high-field intensities, is that the power broadening of the atomic line is stronger in the case of the Gaussian spectrum. In the case of $\beta = 0.1\Gamma$ and $\gamma = 10\Gamma$, the minimum value of the ratio $\langle \sigma'_{22} \rangle / \langle \sigma'_{22} \rangle^L$ is 0.793 ($\langle \sigma'_{22} \rangle^L = 0.385$) and occurs at $\omega_R \approx 4.3\Gamma$. Figure 2 shows the average population $\langle \sigma'_{22} \rangle$ for $\beta = 0.1\Gamma$ (solid line) and $\beta = \infty$ (dashed line) as a function of the detuning, for a Rabi frequency $\omega_R = 10\Gamma$. As we can see, the width of the various resonance curves for $\langle \sigma'_{22} \rangle$ is much larger than the sum of the laser and atomic linewidths, owing to saturation broadening. The broadening is stronger in the case of the Lorentzian spectrum which, because of its higher wings, can cause saturation for detunings larger than those in the case of a Gaussian spectrum. In the case of a Lorentzian spectrum (PDM), the saturation-broadened resonance curve is also Lorentzian and its FWHM is equal to $(\Gamma + \gamma)[1 + 2\omega_R^2/(\Gamma + \gamma)/\Gamma]^{1/2}$. For a Gaussian spectrum we cannot find an analytic expression for the width of the saturation-broadened resonance

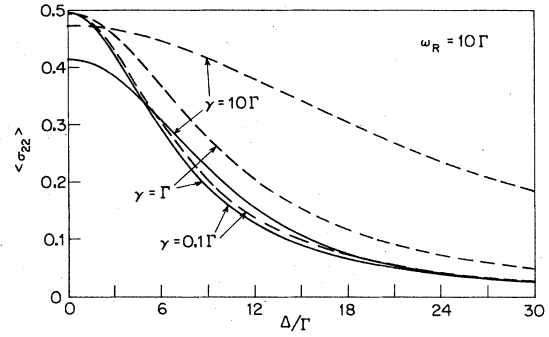


FIG. 2. Plot of the stationary excited-state population $\langle \sigma_{22} \rangle$ for $\beta = \infty$ (dashed line) and $\beta = 0.1\Gamma$ (solid line) versus the ratio of the detuning (Δ) to the spontaneous decay rate (Γ), for a Rabi frequency $\omega_R = 10\Gamma$ and different values of the laser bandwidth (γ).

curve. However, as we see from Fig. 2, for a narrowband spectrum the width is approximately the same for Gaussian and Lorentzian line shapes. It is only in the case of broadband spectrum that the widths are considerably different. For $\gamma = 10\Gamma$, the FWHM of the resonance curve in the case of a Lorentzian spectrum is $\sim 48\Gamma$, while in the case of a Gaussian spectrum it is only $\sim 19\Gamma$.

IV. SPECTRUM OF RESONANCE FLUORESCENCE

As has been shown in the case of exciting fields with Lorentzian line shapes, the spectrum of resonance fluorescence is very sensitive to fluctuations in the exciting field.¹⁻¹⁰ In this section we investigate for the first time the dependence of the emitted spectrum on the laser line shape. The stationary spectrum of the fluorescent light is given by¹⁹

$$S(\omega) = \int_{-\infty}^{\infty} e^{i(\omega - \omega_0)\tau} \langle \hat{\sigma}_{21}(t) \hat{\sigma}_{12}(t + \tau) \rangle dt, \quad (32)$$

where ω_0 is the center frequency of the exciting field and $\langle \hat{\sigma}_{21}(t) \hat{\sigma}_{12}(t + \tau) \rangle = \langle \hat{\rho}_{21}(t) \hat{\rho}_{12}(t + \tau) \rangle e^{i\omega_0\tau}$ the quantum correlation function of the slowly varying atomic raising ($\hat{\sigma}_{21} = |2\rangle\langle 1|$) and lowering ($\hat{\sigma}_{12} = |1\rangle\langle 2|$) operators. This quantum correlation can be calculated by solving the stochastic system of integral equations,⁹

$$g(t + \tau) = \sigma'_{22}(t) e^{(i\Delta - \Gamma/2)\tau} - i\frac{1}{2}\omega_R \int_0^\tau e^{(-i\Delta + \Gamma/2)(t_1 - \tau)} [q(t, t_1) - r(t, t_1)] dt_1, \quad (33)$$

$$f(t, \tau) = \int_0^\tau e^{(i\Delta + \Gamma/2)(t_1 - \tau)} \{-i2\nu(t + t_1)f(t, t_1) + i\frac{1}{2}\omega_R [q(t, t_1) - r(t, t_1)]\} dt_1, \quad (34)$$

$$q(t, \tau) = \int_0^\tau e^{\Gamma(t_1 - \tau)} \{-i\nu(t + t_1)q(t, t_1) - i\frac{1}{2}\omega_R [g(t, t_1) - f(t, t_1)]\} dt_1, \quad (35)$$

$$r(t, \tau) = \sigma'_{21}(t) + \int_0^\tau \{-i\nu(t + t_1)r(t, t_1) + \Gamma q(t, t_1) + i\frac{1}{2}\omega_R [g(t, t_1) - f(t, t_1)]\} dt_1, \quad (36)$$

where

$$g(t, \tau) \equiv \langle \hat{\sigma}_{21}(t) \hat{\sigma}_{12}(t + \tau) \rangle, \quad f(t, \tau) \equiv \langle \hat{\sigma}_{21}(t) \hat{\sigma}_{21}(t + \tau) \rangle e^{-i\omega_0(t + \tau)},$$

$$q(r, \tau) \equiv \langle \hat{\sigma}_{21}(t) \hat{\sigma}_{22}(t + \tau) \rangle e^{-i\omega_0(t + \tau)},$$

and

$$r(t, \tau) \equiv \langle \hat{\sigma}_{21}(t) \hat{\sigma}_{11}(t + \tau) \rangle e^{-i\omega_0(t + \tau)},$$

are quantum correlations, and $\sigma'_{ij}(t) \equiv \langle \hat{\sigma}'_{ij}(t) \rangle$, $i, j = 1, 2$ are quantum averages of the slowly varying elements of the atomic density-matrix operator. Averaging Eqs. (33)–(36) over the frequency fluctuations $\nu(t)$, following the same procedure as in Sec. II, and then taking the Laplace transform with respect to τ we obtain

$$G_N(t, s) = \frac{\langle \sigma'_{22}(t) \rangle_N - i\frac{1}{2}\omega_R[Q_N(t, s) - R_N(t, s)]}{s - i\Delta + \Gamma/2 + N\beta}, \quad (37)$$

$$F_N(t, s) = (i2\{[a(N+1)]^{1/2}F_{N+1}(t, s) + \sqrt{aN}F_{N-1}(t, s)\} + i\frac{1}{2}\omega_R[Q_N(t, s) - R_N(t, s)])/(s + i\Delta + \Gamma/2 + N\beta), \quad (38)$$

$$Q_N(t, s) = (-i\{[a(N+1)]^{1/2}Q_{N+1}(t, s) + \sqrt{aN}Q_{N-1}(t, s)\} - i\frac{1}{2}\omega_R[G_N(t, s) - F_N(t, s)])/(s + \Gamma + N\beta), \quad (39)$$

$$R_N(t, s) = (\langle \sigma'_{21}(t) \rangle_N - i\{[a(N+1)]^{1/2}R_{N+1}(t, s) + \sqrt{aN}R_{N-1}(t, s)\} + \Gamma Q_N(t, s) + i\frac{1}{2}\omega_R[G_N(t, s) - F_N(t, s)])/(s + N\beta), \quad (40)$$

where $G_N(t, s)$, $F_N(t, s)$, $Q_N(t, s)$, and $R_N(t, s)$ are the Laplace transforms of the averages [see Eq. (15)], $\langle g(t, \tau) \rangle_N \equiv \langle g(t, \tau)H_N(\nu(t+\tau)/(\beta\gamma_D)^{1/2}) \rangle$, $\langle f(t, \tau) \rangle_N$, $\langle q(t, \tau) \rangle_N$, and $\langle r(t, \tau) \rangle_N$, respectively. The constant $a = \beta\gamma_D/2$ is the variance of the frequency fluctuations.

The average spectrum $\langle S(\omega) \rangle$ can be obtained from the relation⁹

$$\langle S(\omega) \rangle = G_0(t, i\omega_0 - i\omega) + \text{c.c.} \quad (41)$$

To solve Eqs. (37)–(40) for $G_0(t, s)$ first we eliminate the equation for $G_N(t, s)$ and use the relation $\langle \sigma'_{22}(t) \rangle_N = -i\frac{1}{2}\omega_R[\langle \sigma'_{12}(t) \rangle_N - \langle \sigma'_{12}^*(t) \rangle_N]/(\Gamma + N\beta)$, $t \rightarrow \infty$, to express the stationary averages $\langle \sigma'_{22}(t) \rangle_N$ in terms of $\langle \sigma'_{12}(t) \rangle_N$ and $\langle \sigma'_{12}^*(t) \rangle_N$. Defining then the column vectors $X_N(s) \equiv (\langle \sigma'_{12}(t) \rangle_N, \langle \sigma'_{12}^*(t) \rangle_N, F_N(t, s), Q_N(t, s), R_N(t, s))$ and $Y \equiv i\frac{1}{2}\omega_R(1, 1, 0, 0, 0)$, we can write the matrix recursion relation

$$-i\sqrt{aN}X_{N-1}(s) + b_N X_N(s) - i[a(N+1)]^{1/2}X_{N+1}(s) = Y \delta_{N0}, \quad N=0, 1, 2, \dots, \quad (42)$$

where b_N is a 5×5 complex matrix with elements

$$\begin{aligned} b_N|_{11} &= -b_N|_{22}^* = -i\Delta + \Gamma/2 + N\beta + \frac{1}{2}\omega_R^2/(\Gamma + N\beta), \\ b_N|_{12} &= -b_N|_{21} = -\frac{1}{2}\omega_R^2/(\Gamma + N\beta), \\ b_N|_{33} &= -(s + i\Delta + \Gamma/2 + N\beta)/2, \end{aligned}$$

$$\begin{aligned} b_N|_{34} &= b_N|_{35}^* = i\omega_R/4, \\ b_N|_{41} &= -b_N|_{42} = -b_N|_{51} = -1 + b_N|_{52} \\ &= -\frac{1}{4}\omega_R^2/[(\Gamma + N\beta)(s - i\Delta + \Gamma/2 + N\beta)], \\ b_N|_{44} &= -\Gamma + b_N|_{55} \\ &= -[s + \Gamma + N\beta + \frac{1}{4}\omega_R^2/(s - i\Delta + \Gamma/2 + N\beta)], \\ b_N|_{45} &= -\Gamma + b_N|_{54} = \frac{1}{4}\omega_R^2/(s - i\Delta + \Gamma/2 + N\beta), \\ b_N|_{43} &= -b_N|_{53} = i\frac{1}{2}\omega_R, \end{aligned}$$

and all the other elements being equal to zero. The solution for the column vector $X_0(s) = (\langle \sigma'_{12}(t) \rangle_0, \langle \sigma'_{12}^*(t) \rangle_0, F_0(t, s), Q_0(t, s), R_0(t, s))$ can be written in terms of a matrix continued fraction

$$X_0(s) = \frac{1}{b_0 + \frac{a}{b_1 + \frac{2a}{b_2 + \frac{3a}{b_3 + \dots}}}} Y, \quad (43)$$

from which we can calculate $G_0(t, s)$ using Eq. (37). If $\frac{1}{2}\beta\gamma_D \ll |s + \Gamma + \beta|^2$, $\Delta^2 + (\Gamma/2 + \beta)^2$, and $\omega_R \ll (\Gamma + \beta)$, then it is a good approximation to truncate the continued fraction after b_1 . In this approximation the spectrum of resonance fluorescence is given by

$$\langle S(\omega) \rangle = \left(\frac{\Gamma[-i\Delta(1 - W/(\Gamma + 2\beta)) + (\Gamma + W)/2](s + \Gamma + \frac{1}{2}\gamma_1)(s + i\Delta + \Gamma/2 + 2\gamma_2)}{(\Gamma + W)(s + \frac{1}{2}\gamma_1)p(s)} + \frac{(s + \Gamma + \frac{1}{2}\gamma_1)(s + i\Delta + \Gamma/2 + 2\gamma_2) + \frac{1}{2}\omega_R^2 + \text{c.c.}}{p(s)} \right) \langle \sigma'_{22} \rangle, \quad (44)$$

where

$$p(s) = (s + \Gamma + \frac{1}{2}\gamma_1)(s - i\Delta + \Gamma/2)(s + i\Delta + \Gamma/2 + 2\gamma_2) + \omega_R^2(s + \Gamma/2 + \gamma_2),$$

$$\gamma_1(s) = \gamma_D \frac{\beta}{s + \Gamma + \frac{1}{4}\omega_R^2/(s - i\Delta + \Gamma/2 + \beta) + \beta},$$

$$\gamma_2(s) = \gamma_D \frac{\beta}{s + i\Delta + \Gamma/2 + \beta},$$

with $s = i(\omega_0 - \omega)$. The average population $\langle \sigma_{22} \rangle$ and the parameter W are given by Eqs. (23) and (26), respectively. In the limit of $\beta \rightarrow \infty$, we see that $\gamma_1(s) = \gamma_2(s) = \gamma_D$ and Eq. (44) reduces to the result obtained previously in the case of a phase-diffusion field.¹⁻⁹ The effect of a finite, realistic value for β is that for frequencies $|\omega - \omega_0| \gg \beta$ the effective bandwidths $\gamma_1(s)$ and $\gamma_2(s)$ tend to zero and the spectrum $\langle S(\omega) \rangle$ is the same as in the case

of a monochromatic exciting field. In the case of a strong ($\omega_R \gg \Gamma, \gamma_D$) resonant ($\Delta=0$) field the spectrum exhibits the well-known triplet structure.¹⁹ The positions as well as the widths and heights of the three peaks, which are associated with inelastic scattering, are determined by the roots of the polynomial $p(s)$. In the spectral range $|\omega - \omega_0| \ll \beta$ we can replace $\gamma_1(s)$ and $\gamma_2(s)$ by their values at $s=0$ and the roots of $p(i\omega_0 - i\omega)$ are then given by

$$\omega_1 \simeq \omega_0 - i\frac{1}{2}[\Gamma + 2\gamma_2(0)],$$

$$\omega_{2,3} \simeq \omega_0 \pm \omega_R - i\frac{1}{2}[\frac{3}{2}\Gamma + \frac{1}{2}\gamma_1(0) + \gamma_2(0)].$$

The real parts of the roots correspond to the positions of peaks, while the imaginary parts correspond to their half-widths. The ratio of the height of the center peak at ω_0 to that of the side peaks at $\omega_0 \pm \omega_R$ is $[3\Gamma + \gamma_1(0) + 2\gamma_2(0)]/[\Gamma + 2\gamma_2(0)]$. The integrated spectral intensity of the center peak is $\sim 50\%$ of the total emitted light intensity, the re-

maining 50% being divided equally between the two side peaks. In addition to these three peaks there is also the elastic scattering peak corresponding to the pole at $\omega \simeq \omega_0 - i\frac{1}{2}\gamma_1(0)$ in the first term of Eq. (44). The intensity of the elastic component is, however, negligible for strong incident fields.

As can be seen from the expression for the ratio of the peak heights given above for the case $\omega_R \gg \Gamma, \gamma$, the effect of the laser bandwidth is to decrease the ratio from $3(\gamma_D=0)$ to $\frac{3}{2}(\gamma_D \gg \Gamma)$.¹⁻⁵ Actually, as γ_D increases towards ω_R , the ratio decreases even more to values below unity. That is, the center peak becomes lower than the side peaks, and the spectrum exhibits a center-line dip. This effect was reported in a recent paper,⁹ and it was shown to occur only in the case of phase (frequency) fluctuations (amplitude fluctuations cause the opposite effect). To see the appearance of the center-line dip analytically we consider the special case $\omega_R = \gamma \gg \Gamma/2$, $\Delta=0$, and $\beta \rightarrow \infty$, in which case Eq. (44) reduces to

$$\langle S(\omega) \rangle \simeq \langle \sigma_{22} \rangle \left(\frac{(s + \frac{1}{2}\gamma)(s + 2\gamma) + \frac{1}{2}\omega_R^2}{(s + \frac{1}{2}\gamma)s(s + 2\gamma) + \omega_R^2(s + \gamma)} + \text{c.c.} \right)$$

$$\simeq \frac{2\omega_R^2/(\Gamma + \gamma)}{\Gamma + 2\omega_R^2/(\Gamma + \gamma)} \left(\frac{0.087\gamma}{(\omega - \omega_0)^2 + (1.657\gamma)^2} + \frac{0.199\gamma + 0.373(\omega - \omega_0 + 0.652\omega_R)}{(\omega - \omega_0 + 0.652\omega_R)^2 + (0.421\gamma)^2} \right.$$

$$\left. + \frac{0.199\gamma - 0.373(\omega - \omega_0 - 0.652\omega_R)}{(\omega - \omega_0 - 0.652\omega_R)^2 + (0.421\gamma)^2} \right). \quad (45)$$

The spectrum is symmetric and consists of a broad Lorentzian peak centered at ω_0 , two narrower Lorentzian peaks centered at $\sim \omega_0 \pm 0.652\omega_R$, and two dispersionlike components centered also at $\sim \omega_0 \pm 0.652\omega_R$. The FWHM of the center peak ($\sim 3.3\gamma$) is about four times larger than that of the side peaks (0.84γ), while the height of the side peaks is about 35 times the height of the center peak. The integrated spectral intensity of the center peak is only $\sim 5\%$ of the total emitted light intensity, the remaining 95% being divided equally between the two Lorentzian side peaks. Note that the dispersionlike components have zero integrated intensity and they only serve to redistribute the power from the $|\omega - \omega_0| > 0.652\omega_R$ region into the $|\omega - \omega_0| < 0.652\omega_R$ region of the spectrum. If we take the inverse Fourier transform of Eq. (45)

we find that the stationary correlation $\langle\langle \hat{\sigma}_{21}(t)\hat{\sigma}_{12}(t + \tau) \rangle\rangle$, where the double angular brackets denote both quantum- and classical-field average, is of the form

$$\langle\langle \hat{\sigma}_{21}(t)\hat{\sigma}_{12}(t + \tau) \rangle\rangle = A e^{-a_1|\tau|}$$

$$+ e^{-a_2|\tau|} (B_c \cos b\tau + B_s \sin b|\tau|), \quad (46)$$

with the constants being real positive. The term proportional to $\sin b|\tau|$ gives rise to the two dispersionlike components in the spectrum and vanishes in the case of $\omega_R \gg \gamma, \Gamma$. To explain the difference in the on-resonance spectra for the two cases of $\omega_R \gg \gamma, \Gamma$ and $\omega_R \approx \gamma \gg \Gamma$, we decompose the correlation $\langle\langle \hat{\sigma}_{21}(t)\hat{\sigma}_{12}(t + \tau) \rangle\rangle$ as follows²⁰:

$$\langle\langle \hat{\sigma}_{21}(t)\hat{\sigma}_{12}(t + \tau) \rangle\rangle = \langle\langle \hat{\sigma}'_{21}(t) \text{Re} \hat{\sigma}'_{12}(t + \tau) \rangle\rangle e^{i[\phi(t) - \phi(t + \tau)]} + i \langle\langle \hat{\sigma}'_{21}(t) \text{Im} \hat{\sigma}'_{12}(t + \tau) \rangle\rangle e^{i[\phi(t) - \phi(t + \tau)]}, \quad (47)$$

where $\hat{\sigma}_{21}(t) = \hat{\sigma}'_{21}(t)e^{i\phi(t)}$, $\hat{\sigma}_{12}(t) = \hat{\sigma}'_{12}(t)e^{-i\phi(t)}$, $\text{Re} \hat{\sigma}'_{12} = (\hat{\sigma}'_{12} + \hat{\sigma}'_{21})/2$, and $\text{Im} \hat{\sigma}'_{12} = (\hat{\sigma}'_{12} - \hat{\sigma}'_{21})/2i$. In the case of a monochromatic field ($\phi = \text{const}$), the two components are uncoupled and for $\omega_R \gg \Gamma$, when elastic scattering becomes negligible, we find that^{4,20}

$$\langle\langle \hat{\sigma}_{21}(t) \text{Re} \hat{\sigma}_{12}(t + \tau) \rangle\rangle = \frac{1}{2} \langle\langle \hat{\sigma}'_{22}(t) \rangle\rangle e^{-\Gamma|\tau|/2},$$

$$\langle\langle \hat{\sigma}_{21}(t) \text{Im} \hat{\sigma}_{12}(t + \tau) \rangle\rangle \simeq \frac{1}{2i} \langle\langle \hat{\sigma}'_{22}(t) \rangle\rangle e^{-3\Gamma|\tau|/4} \cos \omega_R \tau.$$

It is clear then that the center peak of the spec-

trum is associated with $\langle \hat{\sigma}'_{21}(t) \text{Re} \hat{\sigma}'_{12}(t + \tau) \rangle$ and the side peaks with $\langle \hat{\sigma}'_{21}(t) \text{Im} \hat{\sigma}'_{12}(t + \tau) \rangle$. We can also see that one-half of the total intensity $\langle \hat{\sigma}'_{22}(t) \rangle$ is in the center peak and the other half in the side peaks. If the phase of the exciting field is fluctuating, then the components $\langle \langle \hat{\sigma}'_{21}(t) \text{Re} \hat{\sigma}'_{12}(t + \tau) \rangle \times e^{i[\phi(t) - \phi(t + \tau)]} \rangle$ and $\langle \langle \hat{\sigma}'_{21}(t) \text{Im} \hat{\sigma}'_{12}(t + \tau) \rangle e^{i[\phi(t) - \phi(t + \tau)]} \rangle$ are coupled. For $\omega_R \gg \Gamma, \gamma$, however, the coupling can be neglected and in the phase-diffusion limit $\beta \rightarrow \infty$ we find that²⁰

$$\begin{aligned} \langle \langle \hat{\sigma}'_{21}(t) \text{Re} \hat{\sigma}'_{12}(t + \tau) \rangle e^{i[\phi(t) - \phi(t + \tau)]} \rangle & \\ \approx \frac{1}{2} \langle \langle \hat{\sigma}'_{22}(t) \rangle \rangle e^{-(\Gamma/2 + \gamma)|\tau|}, & \\ \langle \langle \hat{\sigma}'_{21}(t) \text{Im} \hat{\sigma}'_{12}(t + \tau) \rangle e^{i[\phi(t) - \phi(t + \tau)]} \rangle & \\ \approx \frac{1}{2i} \langle \langle \hat{\sigma}'_{22}(t) \rangle \rangle e^{-3(\Gamma + \gamma)|\tau|/4} \cos \omega_R \tau. & \end{aligned}$$

Therefore, in the case of $\omega_R \gg \gamma, \Gamma$ we can still associate the center peak of the spectrum with one of the components of $\langle \langle \hat{\sigma}'_{21}(t) \hat{\sigma}'_{12}(t + \tau) \rangle \rangle$ and the two side peaks with the other. Moreover, the ratio of the integrated intensities for the center peak and the side peaks is the same as in the case of monochromatic excitation. In the case of $\omega_R \approx \gamma \gg \Gamma$, however, the coupling between the two components of $\langle \langle \hat{\sigma}'_{21}(t) \hat{\sigma}'_{12}(t + \tau) \rangle \rangle$ cannot be neglected. As a result of this coupling, the correlation $\langle \langle \hat{\sigma}'_{21}(t) \text{Re} \hat{\sigma}'_{12}(t + \tau) \rangle e^{i[\phi(t) - \phi(t + \tau)]} \rangle$ develops oscillatory terms and power flows from the center peak out into the side peaks. There is also some power flow towards the center of the spectrum associated with the dispersionlike components in the spectrum. As mentioned earlier, the integrated spectral intensity of the central peak is now only

$\sim 5\%$ of the total intensity while that of the side peaks has increased to $\sim 95\%$. Since $\langle \langle \hat{\sigma}'_{21}(t) \text{Re} \hat{\sigma}'_{12}(t) \rangle \rangle = \langle \langle \hat{\sigma}'_{21}(t) \text{Im} \hat{\sigma}'_{12}(t) \rangle \rangle = \frac{1}{2} \langle \langle \hat{\sigma}'_{22}(t) \rangle \rangle$ and, therefore, each of the two components of $\langle \langle \hat{\sigma}'_{21}(t) \hat{\sigma}'_{12}(t + \tau) \rangle \rangle$, [Eq. (47)], carries half of the total intensity, we can no longer associate a particular spectral component exclusively with either of the two components of $\langle \langle \hat{\sigma}'_{21}(t) \hat{\sigma}'_{12}(t + \tau) \rangle \rangle$. Another important difference between the spectrum for $\omega_R \gg \gamma, \Gamma$ and that for $\omega_R \approx \gamma \gg \Gamma$ is in the widths of the Lorentzian side peaks. In the former case the width is $1.5(\Gamma + \gamma)$ while in the latter it is $\sim 0.84\gamma$, which is less than the laser bandwidth. The narrowing of the side peaks relative to the laser bandwidth is caused by the fact that for $\omega_R \lesssim \gamma \gg \Gamma$, $\Delta = 0$, the atomic dipole cannot follow the fluctuations in the field. As the laser bandwidth is increased, the coherence time of the atomic dipole increases towards the maximum value Γ^{-1} ($\gamma \gg \omega_R, \Gamma$) and the spectrum of resonance fluorescence becomes the same as in the case of spontaneous emission.^{6,21}

Numerical calculations and discussion

We present now some representative results of numerical calculations showing the influence of the laser line shape on the spectrum of resonance fluorescence. As in Sec. III, we consider three different laser line shapes corresponding to $\beta = \infty$, $\beta = \Gamma$, and $\beta = 0.1\Gamma$. The FWHM of each line shape takes three characteristic values: $\gamma = 0.1\Gamma$, $\gamma = \Gamma$, and $\gamma = 10\Gamma$. Figure 3 shows the resonance fluorescence spectra for $\beta = \infty$ (dotted line), $\beta = \Gamma$ (dashed line), and $\beta = 0.1\Gamma$ (solid line), in the case of exact resonance and a Rabi frequency of ω_R

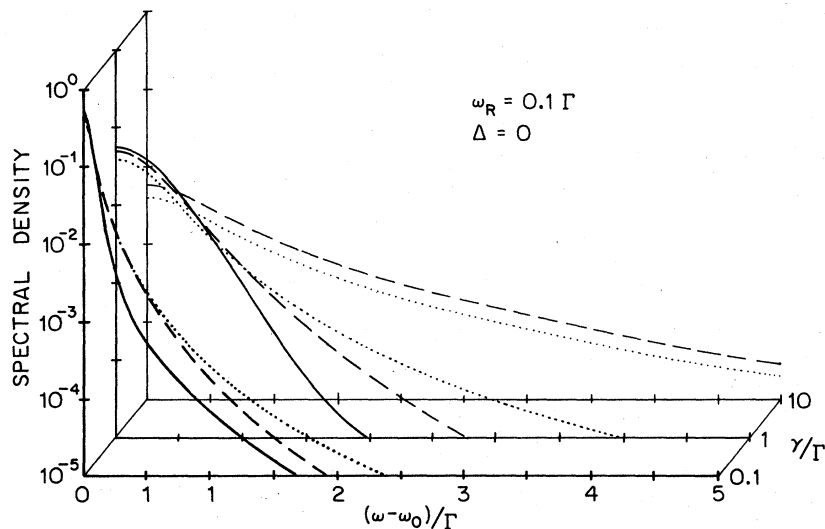


FIG. 3. Resonance fluorescence spectra for $\beta = \infty$ (dotted line), $\beta = \Gamma$ (dashed line), and $\beta = 0.1\Gamma$ (solid line). The values of the Rabi frequency (ω_R), the laser bandwidth (γ), and the detuning (Δ) are given in the figure in units of the spontaneous decay rate (Γ).

$=0.1\Gamma$. The spectra are symmetric about $\omega = \omega_0$ and only the upper half ($\omega > \omega_0$) is shown. At very low Rabi frequencies ($\omega_R \ll \Gamma$) the atom acts like a linear absorber emitter with very low intrinsic quantum noise. Therefore, the spectrum of resonance fluorescence is just the product of the Lorentzian absorption line (FWHM = Γ) with the laser line shape,^{6,21} plus some very low quantum noise. Note that the quantum noise, which is generally a nonlinear function of the incident spectrum, corresponds to inelastic scattering, while the linear and dominant part of the fluorescence spectrum corresponds to elastic scattering. The spectra shown in Fig. 3 are predominantly elastic and to a good approximation, are given by the product of the absorption line and the laser line shape. Notice that for $\gamma = 0.1\Gamma$ the spectra resemble the laser line shapes ($|\omega - \omega_0| < \Gamma$), while for $\gamma = 10\Gamma$ they resemble the absorption line ($|\omega - \omega_0| < \gamma$). Figure 4 shows the spectra in the case of a detuning $\Delta = 5\Gamma$, with all other parameters being the same as in Fig. 3. The elastic part of the spectrum exhibits now two peaks, one at approximately the center laser frequency ω_0 and another at the atomic transition frequency $\omega_{21} = \omega_0 - \Delta$. If $\gamma \ll \Gamma$ then the peak at ω_{21} is negligible, while if $\gamma \gg \Gamma$ then it is the peak at ω_0 that becomes negligible. The inelastic part of the spectrum, on the other hand, exhibits a triplet structure for $\Delta > \gamma$, with a center peak at ω_0 and two side peaks at $\omega_0 \pm (\omega_R^2 + \Delta^2)^{1/2} \approx \omega_0 \pm \Delta$. Although the inelastic part is negligible compared to the elastic part, its contribution is recognizable from the triplet structure of the total spectrum. For $\gamma = 0.1\Gamma$, the

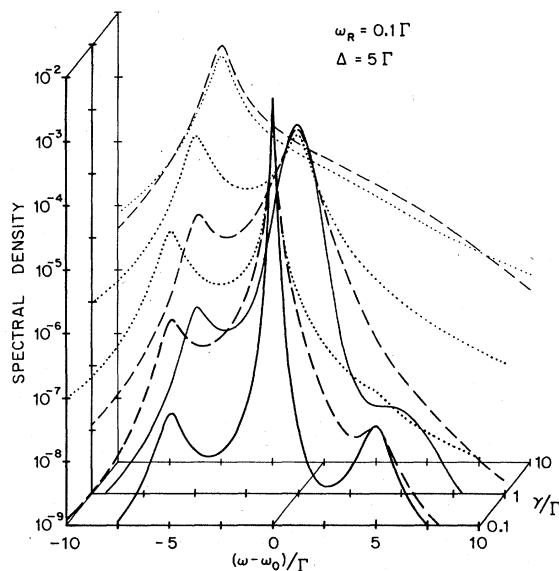


FIG. 4. Resonance fluorescence spectra. Same as Fig. 3 but for a different detuning.

triplet structure is resolved in the case of all three laser line shapes, while for $\gamma = \Gamma$ it is resolved only in the case of the Gaussian line shape ($\beta = 0.1\Gamma$). This shows that as the line shape changes from Gaussian to Lorentzian, or as the laser bandwidth increases, the inelastic component decreases while the elastic increases. It should also be noted that the asymmetry of the spectrum, in the case of off-resonance excitation, becomes less pronounced as the laser line shape changes from Lorentzian to Gaussian. Note also that for $\gamma = 0.1\Gamma$ and $\gamma = \Gamma$, the peak at $\sim \omega_{21}$ in the case of a Lorentzian line shape is about three orders of magnitude higher than in the case of a Gaussian line shape ($\beta = 0.1\Gamma$). This is because the height of the elastic peak at ω_{21} , which is determined by the product of the absorption line peak and the laser spectral density at $\omega = \omega_{21}$, is much larger in the case of a Lorentzian line shape than in the case of a Gaussian line shape. At this point we want to bring attention to some conflicting interpretations. In Refs. 3 and 6, the spectral component referred to herein as elastic peak at ω_{21} is identified as an inelastic component. We should also note that in Ref. 6, the spectral component referred to herein as inelastic part, or quantum noise, is completely neglected. We want to emphasize that the spectral component referred to herein as elastic peak at ω_{21} is associated with elastic scattering and not with inelastic. It arises from linear scattering and does not involve mixing of the incident spectral frequencies. The only difference between the elastic peak at ω_0 and the elastic peak at ω_{21} is that the former is associated with nonresonant scattering while the latter with resonant scattering. In general, the elastic component of the fluorescence spectrum corresponds to light radiated by the quantum-average electric dipole, while the inelastic component corresponds to light radiated by the quantum fluctuations in the dipole.²² That is, if we write $\hat{\sigma}_{21}(t) = \langle \hat{\sigma}_{21}(t) \rangle + \delta \hat{\sigma}_{21}(t)$, where $\langle \hat{\sigma}_{21}(t) \rangle$ and $\delta \hat{\sigma}_{21}(t)$ are the quantum average and fluctuations of $\hat{\sigma}_{21}(t)$, respectively, then the elastic and inelastic and inelastic components are the Fourier transforms of the correlations $\langle \langle \hat{\sigma}_{21}(t) \rangle \langle \hat{\sigma}_{12}(t + \tau) \rangle \rangle$ and $\langle \langle \delta \hat{\sigma}_{21}(t) \delta \hat{\sigma}_{12}(t + \tau) \rangle \rangle$, respectively. The inner brackets in these correlations denote quantum average, while the outer ones denote classical average over the fluctuations in the exciting field. Note that in the limit of very strong fields, when $\langle \hat{\sigma}_{21}(t) \rangle$ vanishes because of saturation, the elastic scattering vanishes as well and all the light is scattered inelastically.²²

Figure 5 shows the resonance fluorescence spectra for a Rabi frequency $\omega_R = 10\Gamma$, with all other parameters being the same as in the case of Fig. 3. The spectra are now predominantly in-

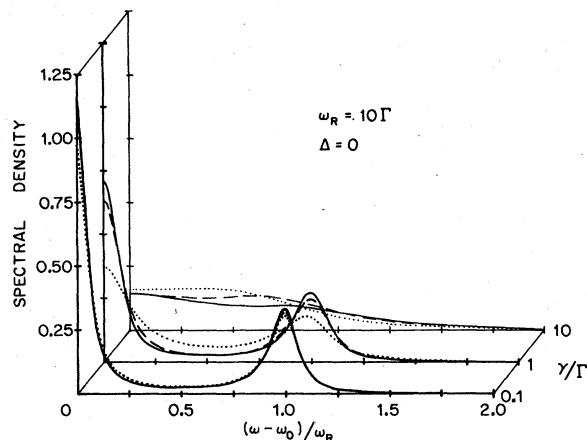


FIG. 5. Resonance fluorescence spectra. Same as Fig. 3 but for a different Rabi frequency.

elastic and for $\gamma < \omega_R$ they exhibit the well-known triplet structure.¹⁹ The effect of the laser bandwidth is to broaden the peaks and reduce the height ratio of the center peak to the side peak. For $\gamma = 0.1\Gamma$ (quasimonochromatic field), the effect of the bandwidth is very small, but we can still see that it depends on the laser line shape. In the case of the Gaussian line shape ($\beta = 0.1\Gamma$, solid line), the center peak and the side peaks are 16.5% and 8.5% higher than the respective peaks in the case of the Lorentzian line shape ($\beta = \infty$, dotted line). For $\gamma = \Gamma$, the broadening and suppression of the peaks become more pronounced and their dependence on the laser line shape is more evident. As discussed earlier, in the case of a Lorentzian line shape (PDM) the widths of the inelastic center peak and side peaks for $\omega_R \gg \gamma, \Gamma$ are $\Gamma + 2\gamma$ and $(3\Gamma + 3\gamma)/2$, respectively. In the case of a Gaussian line shape, numerical calculations for $\gamma = \Gamma$ show that these widths are $\sim \Gamma + \frac{2}{3}\gamma$ and $\sim (3\Gamma + \gamma)/2$, respectively. The center peak and side peaks in the case of the Gaussian line shape are now 90% and 52% higher than the respective peaks in the case of the Lorentzian line shape. It is interesting to mention here that for $\omega_R \gg \gamma \gg \Gamma$, in the limit of $\beta \rightarrow 0$ (ideal Gaussian line shape) the three peaks in the fluorescence spectrum are Gaussian with FWHM equal to γ , and the center- to side-peak height ratio is 2 to 1. Thus, in the case of infinite correlation time for the frequency fluctuations, each of the three peaks reproduces the probability distribution for the random frequency of the exciting field. This should be compared with the other extreme of $\beta \rightarrow \infty$ (ideal Lorentzian line shape), where the three peaks are Lorentzian and the widths of the center peak and side peaks are 2γ and $3\gamma/2$, respectively ($\omega_R \gg \gamma \gg \Gamma$). Note that in this case the center- to side-peak height ratio is 3 to 2. As a final

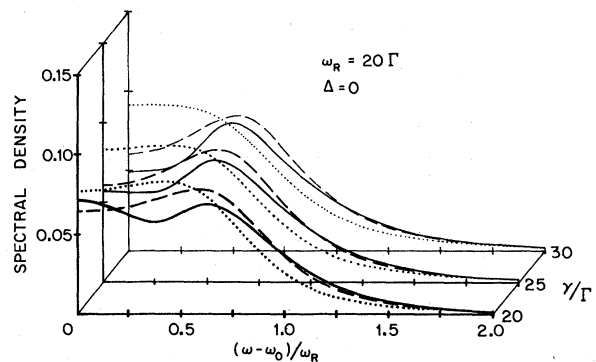


FIG. 6. Resonance fluorescence spectra for $\beta = \infty$ (dotted line), $\beta = 10\Gamma$ (dashed line), and $\beta = \Gamma$ (solid line).

comment on Fig. 5, we should point out that for $\gamma = \Gamma$ the flat-looking fluorescence spectrum in the case of $\beta = \infty$ exhibits a very small (2%) center-line dip.⁹ The other two spectra for $\beta = \Gamma$ and $\beta = 0.1\Gamma$ exhibit strongly broadened triplet structures with the center peak being only a few percent higher than the side peaks.

The development of the center-line dip and its dependence on the laser line shape is shown in more detail in Fig. 6 for a Rabi frequency $\omega_R = 20\Gamma$. The laser line shapes used for this figure correspond to $\beta = \infty$ (dotted line), $\beta = 10\Gamma$ (dashed line), and $\beta = \Gamma$ (solid line). Since the center-line dip appears only for $\gamma \sim \omega_R \gg \Gamma$, we consider in this case the following three values for the laser bandwidth: $\gamma = 20\Gamma$, $\gamma = 25\Gamma$, and $\gamma = 30\Gamma$. One of the things that become clear from Fig. 6 is that, as the laser line shape changes from Lorentzian to Gaussian, the onset of the center-line dip occurs for larger values of the laser bandwidth. At the same time, however, the center-line dip becomes deeper. The reason for the slower development of the dip is that the broadening of the triplet from which it evolves is less for a Gaussian line shape than for a Lorentzian one. On the other hand, the reason for the increased deepening is that the contribution of the side peaks to the spectral density at $\omega = \omega_0$ decreases as the line shape changes from Lorentzian to Gaussian and the side peaks become slimmer. It should also be noted that, as a result of the lesser degree of broadening, the separation between the side maxima is larger in the case of Gaussian line shapes than in the case of Lorentzian line shapes. The difference between the center-line dip and the side maxima in the case of a Lorentzian line shape ($\beta = \infty$) with bandwidth $\gamma = 20\Gamma$ is 7%, while the separation between the side maxima is $\sim 0.8\omega_R$. When the bandwidth of the Lorentzian increases to $\gamma = 30\Gamma$, the center-line dip disappears as the spectral components coalesce into a single line. In contrast, in the case of a line shape with $\beta = \Gamma$ and $\gamma = 30\Gamma$ the

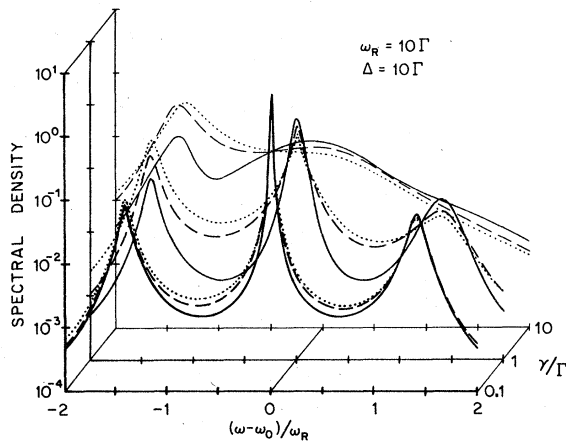


FIG. 7. Resonance fluorescence spectra. Same as Fig. 6 but for different Rabi frequency, detuning, and laser bandwidths.

difference between the dip and the side maxima is 62% and the maxima separation is $\sim \omega_R$. The center-line dip disappears also in the case of $\beta = \Gamma$, but for larger values of the laser bandwidth compared to the case of $\beta = \infty$. Finally, Fig. 7 shows the dependence of the asymmetry of the fluorescence spectrum on the laser line shape, in the case of a detuning $\Delta = 10\Gamma$ and a Rabi frequency $\omega_R = 10\Gamma$. The laser line shapes considered here are the same ones as in Fig. 6. For $\gamma = 0.1\Gamma$ and $\gamma = \Gamma$ the spectra exhibit a triplet structure with a center peak at ω_0 and two side peaks at $\omega_0 \pm (\omega_R^2 + \Delta^2)^{1/2}$. The side peak at $\omega_0 - (\omega_R^2 + \Delta^2)^{1/2}$ is enhanced by the overlap of the laser spectrum with the Stark-shifted component of the atomic transition associated with this particular side peak. This enhancement makes the side peak which is closer to the unperturbed atomic transition frequency higher than the other side peak, and, in

some cases, even the center peak as in the case of $\gamma = \Gamma$. As the line shape changes from Lorentzian to Gaussian, the overlap mentioned above decreases and, therefore, the fluorescence spectrum becomes more symmetric.

In conclusion, we have shown that the laser shape has a strong influence on both the total intensity and the spectral distribution of resonance fluorescence. With regards to the total intensity we have shown the following new result. A Lorentzian line shape, which in the context of our laser model is associated with zero correlation time for the frequency fluctuations, excites more fluorescence than a Gaussian line shape (infinite frequency correlation time) in the case of moderate and strong resonant fields ($\omega_R \gtrsim \Gamma$). This is in contrast to the weak-field case where the situation is reversed. We have also shown that, when the phase fluctuations are correlated (non-Lorentzian line shapes), the intensity of the fluorescence undergoes non-Markovian fluctuations. With regards to the spectrum of resonance fluorescence, we have shown that as the laser line shape changes from Lorentzian to Gaussian the following changes take place: In the case of off-resonance excitation, the asymmetry of the spectrum decreases; in the case of resonant excitation, for $\omega_R \gg \gamma, \Gamma$ the center- to side-peak height ratio increases, while for $\omega_R \sim \gamma \gg \Gamma$ the center-line dip becomes deeper.

ACKNOWLEDGMENTS

This work was supported in part by a grant from the Natural Sciences and Engineering Research Council of Canada, No. A3436, and in part by a grant from the National Science Foundation, No. PHY78-23812.

*Present address: Department of Physics, University of Southern California, Los Angeles, California 90007.

¹G. S. Agarwal, Phys. Rev. Lett. **37**, 1383 (1976).

²J. H. Eberly, Phys. Rev. Lett. **37**, 1387 (1976).

³H. J. Kimble and L. Mandel, Phys. Rev. A **15**, 689 (1977).

⁴P. Avan and C. Cohen-Tannoudji, J. Phys. B **10**, 155 (1977).

⁵P. Zoller and F. Ehlötzky, J. Phys. B **10**, 3023 (1977).

⁶M. G. Raymer and J. Cooper, Phys. Rev. A **20**, 2238 (1979).

⁷A. T. Georges, P. Lambropoulos, and P. Zoller, Phys. Rev. Lett. **42**, 1609 (1979).

⁸P. Zoller, Phys. Rev. A **20**, 1019 (1979).

⁹A. T. Georges, Phys. Rev. A **21**, 2034 (1980).

¹⁰M. Le Berre-Rousseau, E. Ressarye, and A. Tallet, Phys. Rev. A **22**, 240 (1980).

¹¹P. Zoller and P. Lambropoulos, J. Phys. B **12**, L547 (1979).

¹²S. N. Dixit, P. Zoller, and P. Lambropoulos, Phys. Rev. A **21**, 1289 (1980).

¹³H. Haken, in *Handbuch der Physik*, edited by S. Flügge (Springer, Berlin, 1970), Vol. XXV/2c, p. 130.

¹⁴G. E. Uhlenbeck and L. S. Ornstein, Phys. Rev. **36**, 823 (1930); M. C. Wang and G. E. Uhlenbeck, Rev. Mod. Phys. **17**, 323 (1945).

¹⁵A. Papoulis, *Probability, Random Variables and Stochastic Processes* (McGraw-Hill, New York, 1965).

¹⁶*Handbook of Mathematical Functions*, edited by M. Abramowitz and I. A. Stegun (Nat. Bur. Stand., Washington, D. C., 1964).

¹⁷A. T. Georges and P. Lambropoulos, Phys. Rev. A **20**, 991 (1979).

¹⁸The Hermite polynomials $H_N(x)$, as given in Ref. 16,

are not normalized. In this paper we have divided these polynomials by the factors $(2^N N!)^{1/2}$ to make them orthonormal and have modified the recursion relation accordingly.

¹⁹B. R. Mollow, Phys. Rev. A 188, 1969 (1969).

²⁰S. N. Dixit and A. T. Georges (unpublished).

²¹W. Heitler, *The Quantum Theory of Radiation* (Oxford University Press, London, 1954).

²²C. Cohen-Tannoudji, in *Laser Spectroscopy*, edited by S. Haroche *et al.* (Springer, Berlin, 1975).